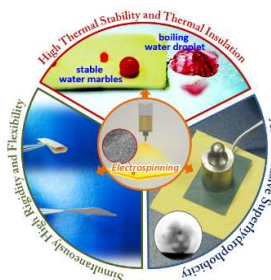


TOC

A Highly Durable Silica/Polyimide Superhydrophobic Nanocomposite Film with Excellent Thermal Stability and Abrasion Resistant Performances

Guangming Gong, Kai Gao, Juntao Wu, Na Sun, Chen Zhou, Yong Zhao*, Lei Jiang*



Superhydrophobic silica/PI nanocomposite film with comprehensive dependent high performances are easily electrospun.

ARTICLE

A Highly Durable Silica/Polyimide Superhydrophobic Nanocomposite Film with Excellent Thermal Stability and Abrasion Resistant Performances

Cite this: DOI: 10.1039/x0xx00000x

Received 00th January 2012,
Accepted 00th January 2012

DOI: 10.1039/x0xx00000x

www.rsc.org/

Guangming Gong^a, Kai Gao^a, Juntao Wu^{*a}, Na Sun^a, Chen Zhou^a, Yong Zhao^{*a}, Lei Jiang^{a,b}

Superhydrophobic self-cleaning materials are widely applicable in many areas, but the poor durability of superhydrophobicity is always the giant obstacles for the real applications of such amazing feature. Here we propose a rather simple way to meet such demanding. We combine the facility of electrospinning and supremacy of polyimide with additional nano-sized silica to afford a durable film with evident self-cleaning feature. Such films presented strong resistance to heat and anti-abrasion property, along-side with perfect thermal insulation. It is a demonstration that the delicate Lotus Effect can also be tough and durable.

Introduction

Lotus leaves have caught people's eyes in the past decades for their interesting surface anti-wetting property¹⁻⁷, which is termed as the Lotus Effect. It gifts a surface with the ability that prevents itself from being contaminated by dirt and dusts. Such superhydrophobic property is quite sought-after in civilian industries, e.g. self-cleaning paints and windows, non-wetting fabrics, anti-icing, and many others.⁸⁻¹⁴ However, self-cleaning surfaces are not so widely applied due to their susceptibility to mechanical abrasion during normal use.¹⁵ Ordinary superhydrophobic surfaces are often easily ruined by either abrasion or heat, because that the surficial micro/nano roughness and/or low surface energy chemicals of a superhydrophobic surface will be destroyed by those two factors. As a result, some superhydrophobic surfaces that can endure abrasions have been created.¹⁶ However, extreme occasions in which heat and abrasions happen simultaneously to the superhydrophobic samples have been seldom addressed. For instances, the natural lotus leaf can be anti-abrasive to some extent by recovering its surface since it is a living organism. Even though, it's still often burned by sunlight because of the thermal lensing effect of the spherical water marble on the leaf surface. Therefore, the good expectation for substantial applications of self-cleaning material conflicts with its own delicacy, resulting in a rather awkward situation.

However, surficial materials of dependable Lotus Effect are quite demanded, especially in some certain areas where harsh conditions, e.g. brutal abrasions and extreme heat, will occur. Notably, NASA has demonstrated the value of Lotus Effect as an effective tool for dust mitigation when astronauts or equipment are conducting extra-vehicular activities on the moon.^{17, 18} Accordingly, if applied as

space suit for lunar exploration, in which temperature variations could be so large (from -173 °C to 120 °C)¹⁹ that plain superhydrophobic materials were likely to fail. Our previous work²⁰ has demonstrated that heat could easily damage normal superhydrophobic plastics, like polystyrene. Therefore, no matter for civil use or for extreme environment, a durable and dependable self-cleaning material with comprehensive high performances needs to be developed.

As a type of super engineering plastics, Polyimide (PI), referring to a polymer family of aromatic imide monomers, is well known for its comprehensive high performance, especially for its great thermal stability and excellent mechanical properties.²¹ On the other hand, Electrospinning, the efficient nanofibers producing method,^{22, 23} has been proved to be a sharp tool for tailoring fine micro structures.²⁴⁻²⁷ In addition, it is also considered as a platform for fabricating multifunctional and hierarchically organized nanocomposite.²⁸ Electrospinning can bring about novel morphologies into PI and the supremacy of PI guarantees the durability of the electrospun products. Their combination provides a potential solution to the foretold problem.

Two factors that govern the superhydrophobicity are low surface energy chemical composition and nano-micro composite surface geometry.²⁹⁻³¹ The later usually turns out to be vulnerable, due to the fine structures can hardly survive from brutal external forces¹⁴ and/or extreme heat²⁰. In other words, the key factor of a durable self-cleaning material lies in the creation and maintaining of its microscopic structures. It is expected that the electrospun PI may defend this challenge. As a result, this work demonstrates meaningful achievement of electrospun polyimide on the preparation of durable self-cleaning materials. In this work, by electrospinning,

we fabricated a nano-silica/PI composite film with robust superhydrophobicity that can endure abrasion and heat, alongside with excellent thermal insulation and fair mechanical performances. These comprehensive performances will greatly broaden the composites' applications in common industry and opened a potential avenue of such dependable self-cleaning surfaces to the applications in extreme conditions.

Experimental

Materials

Nano-sized SiO₂ fillers (hydrophobic) of average primary particle diameter of 40 nm and a specific surface area of 200±50 m²/g were supplied by Degussa (Frankfurt, Germany). Pyromellitic dianhydride (PMDA) and 4,4'-oxydianiline (ODA) were commercial powders. N, N-dimethylformamide (DMF) was stored over 4Å molecular sieves prior to use to minimize the adsorbed water content. 3-aminopropyl triethoxysilane (3-APTS, AR) was purchased from Sigma-Aldrich and used without further treatment.

Synthesis of PAA and the Nano-sized SiO₂/PAA System

The synthesis follows the traditional route of solution polymerization from PMDA and ODA in DMF, as demonstrated in Scheme S1. The synthetic procedure was as follows: First, a pre-calculated amount of nano-sized SiO₂ filler was added into DMF solution and then ultra-sonication was applied to the mixture for 30 min. 3-APTS was added in after 10 min of the above step. The SiO₂/DMF solution and ODA were added into a three-necked flask with a stirrer. After thorough mixture, equal molar amount of PMDA was added in to afford polyamic acid (PAA). The suspension was vigorously stirred for a further 4h at cryogenic environment to yield a sticky mixture. And the following affording of PI by thermal imidization could also be referred to Scheme S1.

Preparations of composite *via* electrospinning

Neat membranes were yielded by casting PAA or the SiO₂/PAA hybrid solution on clean glass pieces, and then converted into PI membranes by thermal imidization. To fabricate the electrospun mat, 2 ml of the PAA or SiO₂/PAA solution was added in plain plastic syringes connected by a metal nozzle with inner diameter of 0.8mm. Then an 18 kV voltage (DW-N303-1AC D8, Dongwen High Voltage Supplier, Tianjin, China) was applied on the nozzles. Constant air pressure was applied onto the solution to guarantee its outflow rate was as steady as 0.5ml/s. The electrospun substances were collected by a flat metal collector (alumina foil) opposite to the nozzle and the distance between the nozzle tips to the collector was about 15 cm. After 1h, the as-spun non-woven-mat-like samples were carefully ripped off from the foil. A follow imidization would afford them into silica/PI composites. During the electrospinning process, the temperature and relative humidity were fixed at 45 °C and 30%.

Characterization

Surface morphologies of the membranes were studied by a scanning electron microscopy (SEM, JSM-6700F, JEOL, Japan). Water CA was measured on a CA system (OCA20, Dataphysics, Germany) at ambient temperature. Each sample was measured five times and an average value of adhesion was given. Tensile testing of the as-spun mats was conducted on a tensile testing machine (AGX-S, ShimadzuTM, Japan). The stretching rate was 1mm/min. Data was given in the form of Load-Distance. Then it was converted into Stress-Strain curve by mathematical calculation. Thermal conductivity of the samples were examined by a Hot DiskTM multi-functional thermal conductivity testing machine. The testing mechanism was based on the Transient Plane Source Method.

Results and Discussion

Design and Preparation of the Electrospun Mat with Lotus Effect

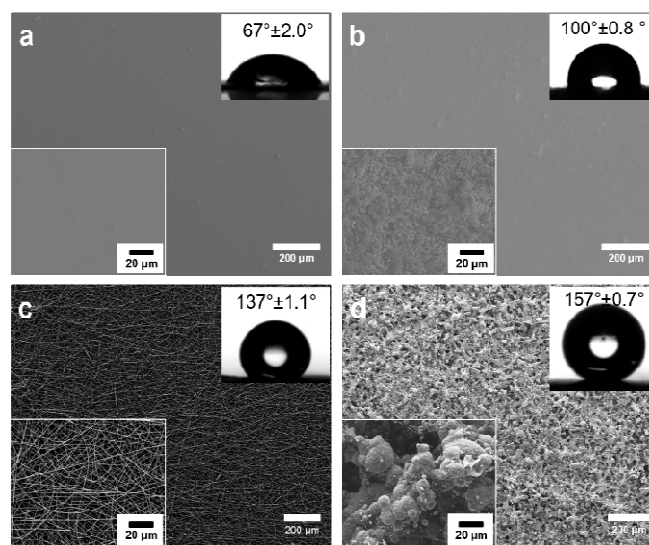


Figure 1. SEM and wettability characterizations of four different types of polyimide films. (a) surficial characterization of a casted neat PI film; (b) surficial morphology of a casted silica/PI film with silica content of 30 wt%; (c) surficial structure of the electrospun PI mat; (d) surficial structure of an electrospun silica/PI hybrid film. Contact angles of 3μL water droplets on each sample are inserted.

Lotus Effect mainly involved two aspects: superhydrophobicity and low liquid/solid interface adhesion.²⁹ Both of these two factors were governed by surface energy and surface geometrical microstructures.^{29, 31} The major principles to realize superhydrophobic self-cleaning surfaces are always to lower the free-energy and increase the fine roughness of the solid phase. In our work, the lowering of PI's surficial energy could be achieved by doping nano-sized silica via in-situ polymerization (Scheme S1). And the composite's hierarchical nano-micro roughness was constructed by electrospinning.

Figure 1a showed the smooth surface morphology of a casted PI film. The insertion showed its intrinsic CA of 67°±2.0°, which met PI's weak hydrophobicity. After the introduction of silica nanoparticles, the casted composite's CA increased to 100°±0.8°, as shown in Figure 1b. The hydrophobic silica particles seized some

positions on the surface of the film, which triggered the increase of the composite's CA, proving the addition of silica was helpful to the lowering of the surface free-energy. In Figure 1c, pure PI was electrospun into non-woven mat, which was consisted of nanofibers. By comparing the morphologies in Figure 1a and 1c, the micro roughness brought by electrospinning was greatly enhanced, which was in favour of hydrophobicity. And the CA of pure PI rose from $67^{\circ} \pm 2.0^{\circ}$ to $137^{\circ} \pm 1.1^{\circ}$. Such fact was a strong proof of that the enhancement of micro roughness was also benefit for amplifying PI's repellency to water. To further realize PI mat's superhydrophobicity, we intended to use the combined strategies. Therefore, a series of electrospun nano-composites containing different amount of nano silica were prepared. The experimental results showed that the composite with a silica content of 30 wt% presented the most ideal features, whose surface structure was illustrated in Figure 1d. The SEM photo demonstrated a highly porous structure with nano-sized silica embedded on the surface of the resin (Figure 1d enlargement). The formation mechanism was illustrated and discussed in Figure S2. The hybrid nanocomposite mat behaved typical Lotus Effect. The static water contact angles on it were as high as $157^{\circ} \pm 0.7^{\circ}$ and water droplets even as small as 3 μL rolled off easily. An animation of water rolling effect can be checked in the supporting information. Conclusively, the addition of nano-sized hydrophobic silica and the hierarchical roughness brought by electrospinning gave rise to the composite's final slippery superhydrophobicity. Films with lower or higher content of silica were either not superhydrophobic or not free-standing (referred in Supporting Information, Figure S1). Therefore, the 30 wt% loaded silica/PI hybrid films were further studied in the following experiments.

Thermal Stability of the Electrospun Nanocomposite

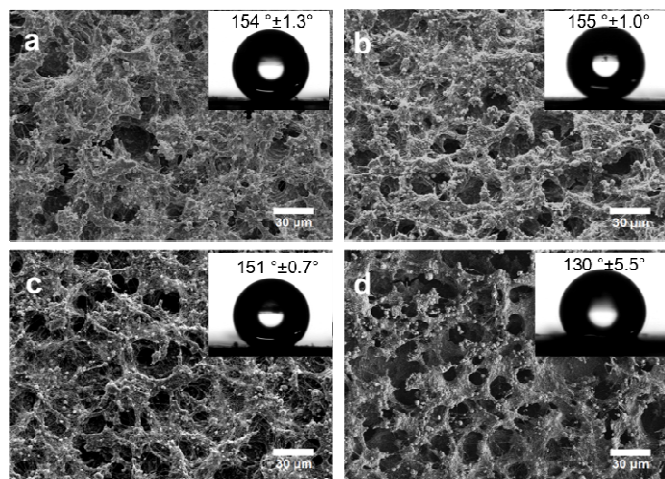


Figure 2. SEM characterizations of the 30 wt% silica/PI hybrid film treated at different temperatures. (a) surficial structure of an untreated sample; (b) surficial structure of a sample treated at 350°C ; (c) surficial structure of a sample treated at 400°C ; (d) surficial structure of a sample treated at 450°C . After thermal treatment and when the samples were cooled down, the wettability of each sample were examined and the contact angles were given as insertions.

Because of PI's outstanding thermal stability, we expected the nanocomposite film was also thermal stable and could maintain its superhydrophobicity after thermal treatment. Therefore, thermal treatments were carried out to study the nanocomposite's stability against the heat. The sample was cut into pieces and were placed into an oven, treated in ambient air atmosphere. The heating rate was about $10^{\circ}\text{C}/\text{min}$. After heated to the target temperature, the temperature was fixed for 30min. Thermal treating temperatures were set at 300°C , 350°C , 400°C and 450°C , respectively. Here, it was noted that the as-spun silica/PAA precursor was imidized at 300°C to afford silica/PI composite. So that the beginning thermal-treat temperature was set at 300°C . After cooled down to room temperature, the CAs of each sample were examined, alongside with the sliding angles. Even when the treated temperature was up to 400°C , as we found, the superhydrophobicity nanocomposite still reserved its self-cleaning ability well.

Such nicely reserved surficial property was attributed to the fact that PI and silica's excellent thermal stability prevented the micro structures of the samples from being damaged by heat. TGA analysis of the 30 wt% loaded silica/PI was given in Figure S3 and it indicated excellent thermal stability of such nanocomposite. In Figure 2b and Figure 2c, the SEM photos proved that the electrospun morphology of such composites could be well maintained after the heat test at corresponding temperatures. However, when treating temperature reached 450°C , which was above PI's T_g , the overwhelmingly high heat damaged its original surficial morphology, resulted in the loss of superhydrophobicity. Based on these data, herein we safely concluded that the working temperature limitation of this superhydrophobic film could be as high as 400°C . Consequently, we believe the enduring nanocomposite with such a thermal stable superhydrophobicity can meet application requirements where extreme heat may take place.

Mechanical performance of the Silica/PI composite film

The mechanical performances of the silica/PI composites were examined. As comparison, the mechanical behaviours of the electrospun neat PI non-woven mats were also tested. Generally, the stress of the composites were 26.9 ± 1.1 MPa and the maximum strains were 7.2 ± 1.2 %. Meanwhile the corresponding data of the non-woven mats were 13.2 ± 2.3 MPa and 12.0 ± 4.5 %. Two typical stress-strain curves representing the two kinds of samples were given in Figure 3a, respectively. Clearly, the introduction of inorganic silica nano particles endowed the composite with greater rigidity. The stress enhancement of the polymers caused by the incorporations of inorganic nano fillers e.g. carbon tubes, nano diamonds, silica, etc., were commonly seen in the preparations of electrospun nano composites.³²⁻³⁷ The enhanced rigidity of the silica/PI composite enabled itself stiff enough to stand its own weight, as show in Figure 3b. Yet, the rigidity-enhancement did not sacrifice the composite's flexibility. As can be seen from Figure 3d, a small piece of silica/PI composite sized in 2×2 cm^2 , was able to suffer from the fierce bending force without cracking. Such property could make the thin composite more easy-handling than the pliable neat nonwoven mat when being operated. It was noteworthy that according to the stress-strain curve, the moduli of the two

electrospun samples varied in the initial stretching process, as shown in the insertion of Figure 3a. At the beginning of the stretching, due to electrospun nonwoven formations, these samples were easily

deformable so that the moduli of the samples were low, 58.67 MPa for the composites and 60.25 MPa for the mat, respectively. As the stretching went on, the fibrous structures

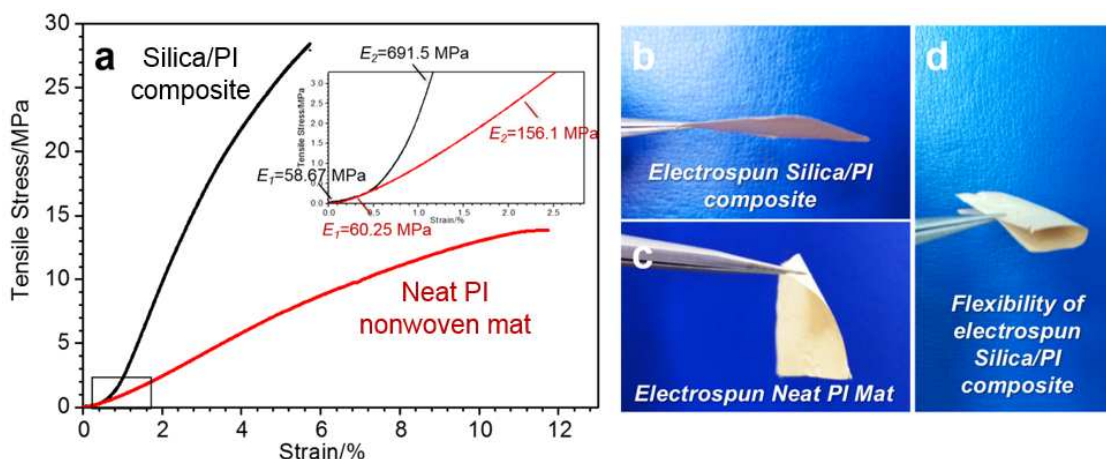


Figure 3. Mechanical performance of the silica/PI composite and the comparison between the composite and the neat PI nonwoven mat. (a) stress-strain curve of the electrospun silica/PI composite (black) and the neat PI non-woven mat (red). the insertion is the magnification of the initial part of the stress-strain curve, in order to illustrate the moduli variations; (b) display of the rigidity of the composite film; Compared to (c) a pliable neat electrospun PI mat, the silica/PI composite film presented higher rigidity, and (d) simultaneously, with considerable flexibility.

tended to be aligned in the stretching direction and became less deformable. Then the samples' moduli increased to 691.5 MPa and 156.1 MPa. Such buffering effect made the electrospun composite less sensitive to abrupt forces and more dependable.

Anti-abrasion feature of the Silica/PI composite mat

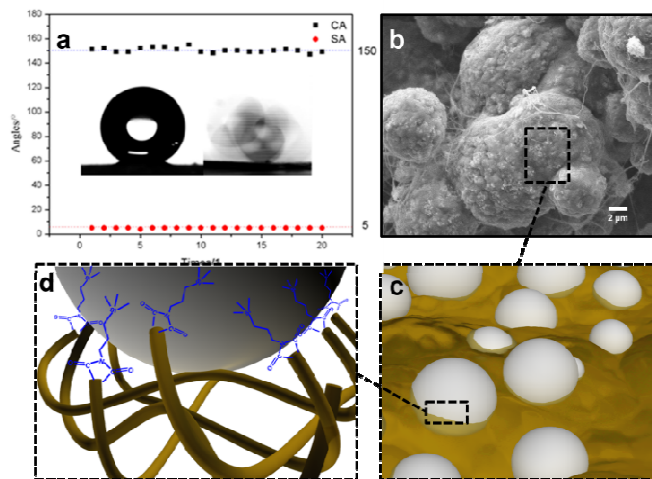


Figure 4. (a) Contact angles and sliding angles (part) plotted after each abrasion and the insertions are static image of a 5 μ L water droplet showing a high contact angle and a snapshot of a rolling water droplet, respectively; (b) SEM characterization of the hybrid film's surface structure after the abrasion test, showing no obvious change of the original morphology; (c) Computer graphical illustration of the specific area of b), indicating that the nano silica (white spheres) were firmly embedded onto the yellow PI resin; (d) Schematic illustration of the chemical bonding of the 3-APTS between the polymer chains and surface of the SiO₂ particles (also discussed in S.I.).

Since the superhydrophobicity was triggered by the micro-nano structures, the reservation of these fine structures after external physical contact was of great importance to the maintaining of surface wetting property. In order to investigate the hybrid film's self-cleaning property against external forces, an abrasion test was carried out. We used an abrasive paper to scratch the surface of the as-spun nanocomposite and following tests of water CA and SA were conducted. The abrasion test method was discussed in detail in Figure S5. As shown in Figure 4a, the CA kept staying above approximately 150° and the SA under 5° after multiple times of scratch (only part of the data was shown in Figure 4a. The surface morphologies of the film was re-characterized after the abrasion test.

Figure 4b displayed that the embedded silica on the PI resin were well reserved, which was schematically illustrated in Figure 4c. Firstly, as we mentioned, PI was mechanically strong and could form tough polymer matrix to maintain a durable micro structure. Additionally, during the polymerization, the coupling agent, 3-aminopropyl triethoxysilane (3-APTS) was added to enhance the bonding between the resin and the inorganic particles. Schematic bonding mechanism could be described as in Figure 4d. The chemical bonding could be referred in supporting information (Figure S4). As a result, these two factors prevented the nano-silica from being peeled-off by external forces and simultaneously kept the original micro structures of the film, ensuring the robustness of the superhydrophobicity.

Thermal-insulation of the hybrid film

Thermal insulation is an important aspect of materials. Here, by combining the thermal advantages of silica and PI, the electrospun composite film can meet the requirement. The thermal conductivity

ARTICLE

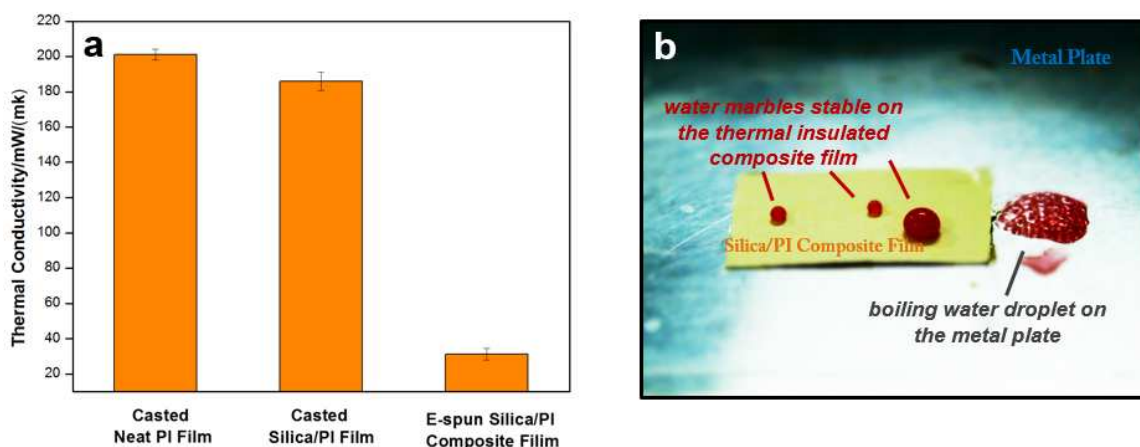


Figure 5. (a) Thermal conductivity chart of three types of films and (b) a demonstration of the thermal insulated superhydrophobic silica/PI composite applying on a hot metal plate. Water marbles were dyed in red for better discernibility. Water droplets on the yellow composite mat maintained superhydrophobicity in spite of the heat, while on the heated metal plate, water droplet was boiling and evaporated rapidly. This photo was a snapshot from the video in the supporting information. Only colour tones, brightness and contrast were adjusted via Photoshop in order to convey a better viewing.

data in Figure 5a showed that the thermal conductivity of the hybrid composite was as low as 31.2 ± 3.2 mW/m·K. Such excellently low thermal conductivity could be contributed to the combination of electrospinning and silica. The original conductivity of the casted PI film was 201.0 ± 3.0 mW/(m·K). After 30 wt% silica was doped in, the casted hybrid film's heat conductivity was lowered to 185.9 ± 5.3 mW/(m·K). The introduction of silica was helpful to lower the conductivity of the system for it had created numerous silica-PI interfaces across the whole film. And these interfaces could cause considerably large energy dissipations. After the mixture was electrospun, the conductivity of the composite film dropped sharply to 31.2 ± 3.2 mW/(m·K). Such evident drop of thermal conductivity lay in the fact that numerous micro spaces were introduced into the system during the electrospinning. From the previous comparison of SEM characterizations, the micro structures of electrospun film and the casted film were totally different. In the casted film, the whole structure was an integrated entity. The thermal-conduct paths were continuous. However, in the electrospun film, the existence of those micro pores resulted in discontinuous thermal conduct paths which in turn gave the composite film an ultralow thermal conductivity. Such low thermal conductivity was mighty enough to prevent the heat of fire from damaging the composite film's surficial superhydrophobicity. And such heat-proof superhydrophobicity was especially crucial to self-cleaning materials when applied on a hot body or against hot environment. The video demonstrating such ability could be found in the supporting information (see the second movie). As displayed in Figure 5b, which was a snap-shot of the video, the silica/PI composite film was placed onto a metal plate heated by a fire underneath. Water droplets were dipped onto the composite and metal plate, respectively. After a few seconds, water

on the metal plate started to boil and evaporated violently. While on the composite film, the water marbles stayed steadily, without being affected by the heat of fire.

Conclusions

The silica/PI nanocomposite film with durable superhydrophobicity was fabricated via a simple electrospinning method. Its robust superhydrophobicity could endure extreme heat and considerable physical abrasions. Additionally, the high porosity and well coupling of nano-sized silica endowed this composite with good mechanical performances and ultra-low thermal conductivity. These comprehensive practical properties of the nanocomposite made an evident proof that the traditionally-thought delicate Lotus Effect could also be as tough as possible, paving its way into applications where harsh conditions would take place.

Acknowledgement

The work is financially supported by the National Natural Science Foundation of China (No.51373007, 51003004), the Beijing Natural Science Foundation (No.2142019), the National Basic Research Program of China (No.2010CB934700, 2012CB933200), the Fundamental Research Funds for the Central Universities, and the SRF for ROCS, SEM

Notes and references

^a Key Laboratory of Bio-Inspired Smart Interfacial Science and Technology of Ministry of Education, School of Chemistry and

Environment, Beihang University, No. 37 Xueyuan Rd., Beijing, 100191, P.R. China. E-mail: wjt@buaa.edu.cn; zhaoyong@buaa.edu.cn

^b Beijing National Laboratory for Molecular Sciences (BNLMS), Institute of Chemistry, Chinese Academy of Sciences, Zhongguancun North First Street 2, Beijing, 100190, P.R. China

† The manuscript was written through contributions of all authors. All authors have given approval to the final version of the manuscript. The authors G. Gong and K. Gao contributed equally to this work.

Electronic Supplementary Information (ESI) available: Synthetic route of PI and Silica/PI, SEM characterizations of composites with different content of silica, structural formation mechanism of the electrospun film, TGA of silica/PI composite, speculation of coupling mechanism of 3-APTS, display of the abrasion test, videos of water-rolling and fire-proof superhydrophobicity of the nanocomposite. See DOI: 10.1039/c000000x/

- 1 L. Feng, S. Li, Y. Li, H. Li, L. Zhang, J. Zhai, Y. Song, B. Liu, L. Jiang and D. Zhu, *Adv. Mater.*, 2002, **14**, 1857
- 2 A. Marmur, *Langmuir*, 2004, **20**, 3517
- 3 N. A. Patankar, *Langmuir*, 2004, **20**, 8209
- 4 H. J. Lee and S. J. Michielsen, *Text. Inst.*, 2006, **97**, 455
- 5 Y. T. Cheng, D. E. Rodak, C. A. Wong and C. A. Hayden, *Nanotechnology*, 2006, **17**, 1359
- 6 Y. Li, G. Duan, G. Liu and W. Cai, *Chem. Soc. Rev.*, 2013, **42**, 3614
- 7 Y. Li, W. Cai, B. Cao, G. Duan, F. Sun, C. Li and L. Jia, *Nanotechnology*, 2006, **17**, 238
- 8 X. Zhang, F. Shi, J. Niu, Y. Jiang and Z. Wang, *J. Mater. Chem.*, 2008, **18**, 621
- 9 X. Gao, X. Yan, X. Yao, L. Xu, K. Zhang, J. Zhang, B. Yang and L. Jiang, *Adv. Mater.*, 2007, **19**, 2213
- 10 X. Li, D. Reinhoudt and M. Grego-Calama, *Chem. Soc. Rev.*, 2007, **36**, 1350
- 11 J. Genzer and K. Efimenko, *Biofouling*, 2006, **22**, 339
- 12 P. Joseph, C. Cottin-Bizonne, J. M. Benoit, C. Ybert, C. Journet, P. Tabeling and L. Bocquet, *Phys. Rev. Lett.*, 2006, **97**, 156104
- 13 H. Y. Erbil, A. L. Demirel, Y. Avci and O. Mert, *Science*, 2003, **299**, 1377
- 14 A. R. Parker and C. R. Lawrence, *Nature*, 2001, **414**, 33
- 15 X. Zhu, Z. Zhang, X. Men, J. Yang, K. Wang, X. Xu, X. Zhou and Q. Xue, *J. Mater. Chem.*, 2011, **21**, 15793
- 16 Q. Xu, B. Mondal and A. M. Lyons, *ACS Appl. Mater. Interf.*, 2011, **3**, 3508
- 17 D. Cadogan and J. Ferl, *SAE Technical Paper*, 2007
- 18 D. V. Margiotta, W. C. Peters, S. A. Straka, M. Rodriguez, K. R. McKittrick and C. B. Jones, *Proc. of SPIE*, 2010, **7794**, 77940I-1
- 19 J. C. Jaeger, *Aust. J. Phys.*, 1953, **6**, 10-21.
- 20 G. Gong, J. Wu, J. Liu, N. Sun, Y. Zhao and L. Jiang, *J. Mater. Chem.*, 2012, **22**, 8257
- 21 I. Yoshio and Y. Rikio, *Saishin Polyimide, Kiso to Ouyou*, NTS Inc., 2002
- 22 D. Li and Y. Xia, *Adv. Mater.*, 2004, **16**, 1151
- 23 A. Greiner, J. H. Wendorff, *Angew. Chem. Int. Ed.*, 2007, **46**, 5670
- 24 B. Almería, W. Deng, T. M. Fahmy and A. Gomez, *J. Colloid Interf. Sci.*, 2010, **343**, 125
- 25 E. Scholten, H. Dhamankar, L. Bromberg, G. C. Rutledge and T. A. Hatton, *Langmuir*, 2011, **27**, 6683
- 26 Z. Chang, *Chem. Commun.*, 2011, **47**, 4427-4429
- 27 K. Hayashi, K. Ono, H. Suzuki, M. Sawada, M. Moriya, W. Sakamoto and T. Yogo, *Small*, 2010, **6**, 2384
- 28 W. E. Teo, S. Ramakrishna, *Compos. Sci. Technol.*, 2009, **69**, 1804
- 29 M. Liu and L. Jiang, *Adv. Funct. Mater.*, 2010, **20**, 3753
- 30 X. Liu, Y. Liang, F. Zhou and W. Liu, *Soft Matter*, 2012, **8**, 2070
- 31 M. Liu, Y. Zheng, J. Zhai and L. Jiang, *Acc. Chem. Res.*, 2010, **43**, 368
- 32 E. Reynaud, T. Jouen, C. Gauthier, G. Vigier and J. Varlet, *Polymer*, 2001, **42**, 8759.
- 33 D. Chen, T. Liu, X. Zhou, W. Liu, H. Hou, *J. Phys. Chem. B*, 2009, **113**, 9741
- 34 L. Liu, M. Eder, I. Burgert, D. Tasis, M. Prato and H. D. Wagner, *Appl. Phys. Lett.*, 2007, **90**, 083108
- 35 J. J. Ge, H. Hou, Q. Li, M. Graham, A. Greiner, D. H. Reneker, F. W. Harris and S. Z. D. Cheng *J. Am. Chem. Soc.*, 2004, **126**, 15754
- 36 K. D. Behler, A. Stravato, V. Mochalin, G. Korneva, G. Yushin and Y. Gogotsi, *ACS Nano*, 2009, **3**, 363-369
- 37 S. Cheng, D. Shen, X. Zhu, X. Tian, D. Zhou and L. Fan, *Euro. Polym. J.*, 2009, **45**, 2767